Surface morphology and electronic structure of bulk single crystal β-Ga_2O_3(100)

T. C. Lovejoy,[1,a)] E. N. Yitamben,[1] N. Shamir,[1,b)] J. Morales,[1,c)] E. G. Villora,[2] K. Shimamura,[2] S. Zheng,[3] F. S. Ohuchi,[3] and M. A. Olmstead[4]
[1]*Department of Physics, University of Washington, Seattle, Washington 98195, USA*
[2]*National Institute for Materials Science, Tsukuba, Japan*
[3]*Department of Materials Science and Engineering, University of Washington, Seattle, Washington 98195, USA and Center for Nanotechnology (CNT), University of Washington, Seattle, Washington 98195, USA*
[4]*Department of Physics, University of Washington, Seattle, Washington 98195, USA and Center for Nanotechnology, University of Washington, Seattle, Washington 98195, USA*

(Received 21 November 2008; accepted 2 February 2009; published online 26 February 2009)

Experimental studies of the surface morphology and electronic structure of bulk single crystals of the transparent and wide gap semiconductor gallium oxide (β-Ga_2O_3) have been conducted using scanning tunneling microscopy (STM), low-energy electron diffraction (LEED), and angle-resolved photoemission spectroscopy (ARPES). Atomically resolved STM and LEED results for the β-Ga_2O_3(100) surface clarify that the predominant surface termination contains both gallium and oxygen, and this surface does not exhibit a reconstruction. The valence band structure was obtained with ARPES and shows good agreement with existing theoretical works at the zone center and along the a^* and c^* directions, except that the calculated bandwidth is ~7% too small. There is poorer agreement along the b^* direction, where the experimental bands disperse more strongly than the calculations. © *2009 American Institute of Physics*. [DOI: 10.1063/1.3086392]

Technological uses of oxides include catalysts, gas sensors, and transparent conductors, to name a few.[1] While there is a relatively large body of surface science literature on thin metal oxide films, very few bulk single crystal oxide surfaces have been studied. The most work has been done on TiO_2,[2] then ZnO,[3] and while surface studies of oxides of main group elements other than Al_2O_3 exist,[4] they are scarce. This is at least partially due to the technical difficulty of applying electron-based techniques to bulk oxides because of charging effects arising from the typically low conductivity. In particular, the surface sensitive techniques scanning tunneling microscopy (STM) and angle-resolved photoemission spectroscopy (ARPES) are practically difficult to apply, while the amount that can be learned from them is quite large.

The β phase of the wide gap (4.9 eV) (Ref. 5) semiconductor β-Ga_2O_3 is reported to be the only stable form of gallium oxide at all temperatures up to the melting point at 1800 °C.[6] The complex crystal structure is base centered monoclinic with lattice parameters a=12.23 Å, b=3.04 Å, c=5.80 Å, and β=103.7° (between a and c). A good visualization is given in Ref. 7. The surface of single crystal β-Ga_2O_3 has been studied with atomic force microscopy (AFM)[8,9] where uniform step heights corresponding to half the unit cell were observed, and thin films obtained by oxidizing CoGa have been studied with STM and low-energy electron diffraction (LEED);[10,11] however, atomic resolution information on single crystal Ga_2O_3 has not been reported. This transparent material is an intrinsic insulator, but displays n-type semiconductor behavior when prepared under some conditions.[12] Amorphous gallium oxide films[13] and single crystals[14] have been proposed as high-temperature gas sensors whose conductivity varies with the partial pressure of oxidizing or reducing gases. Crystalline β-Ga_2O_3 has also been used as a substrate for epitaxial growth of GaN[15] and is a promising material for optoelectronics devices as a transparent conducting oxide due to its transparency in the near-UV.[16]

In this letter, we report on the application of STM, LEED, and ARPES to bulk single crystals of β-Ga_2O_3. STM and LEED reveal the local structure of the (100) or bc plane of Ga_2O_3 to be unreconstructed. The measured electronic band structure is in qualitative agreement with published theoretical calculations,[17,18] although some significant differences are observed.

Single crystals of β-Ga_2O_3 were grown by the floating zone technique in Japan[12] starting from powders of 99.99% purity. Ultrahigh vacuum (UHV) STM, LEED, and conductivity measurements were conducted using a commercial surface science instrument (Omicron). Room temperature photoemission experiments were conducted at the Advanced Light Source (ALS), Beamline 7.0.1, utilizing a hemispherical Scienta R4000 spectrometer and photons linearly polarized perpendicular or nearly perpendicular to the c direction in the energy range of 80–130 eV. Temperatures were recorded with an optical pyrometer. Crystalline samples roughly $1\times3\times10$ mm^3 were cleaved from a large single crystal and mounted on a sample holder designed to pass current through the sample via Ta clips pressed in mechanical contact with it. Resistance measurements were made in this arrangement with a digital multimeter (Fluke 75). Samples were placed in a conductive state for STM and photoemission experiments by the application of a voltage pulse through the sample (200–400 V, 1–2 s across the 10 mm sample) drawing less than 0.1 A. After prolonged heating

a)Electronic mail: tlovejoy@u.washington.edu.
b)On sabbatical leave from Nuclear Research Center-Negev, Beer-Sheva, Israel.
c)Present address: Department of Physics, University of Illinois, Urbana, Illinois 61801.

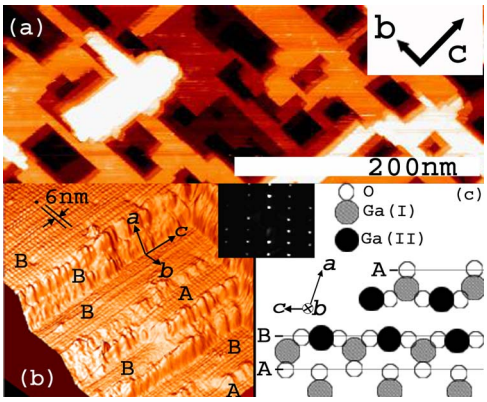

FIG. 1. (Color online) (a) STM image showing five terrace levels vertically spaced by ~5.9 Å on the Ga_2O_3 (100) surface. (b) 3D perspective view STM image showing atomic level corrugation on both the B and A terminations (STM parameters: V_{tip}=−7 V,0.2 nA). (c) Schematic diagram of β-Ga_2O_3 lattice viewed along the *b* axis shows that A-B step height is larger than that of B-A by about one Ga(II)–O bond (~2 Å). (inset) LEED showing 1×1 rectangular pattern corresponding to unreconstructed *b* (horizontal) and *c* (vertical) axes.

around 800–1000 °C by direct current in UHV (30–50 V, 0.3–0.5 A, 20–200 min), found necessary for obtaining good surface order in STM, the sample would revert to a relatively insulating state and another voltage pulse would be required to achieve conduction. In this configuration it is difficult to separate the relative contribution to the total resistance of sample conductivity and nonohmic contacts.

The local structure and surface morphology were studied with STM after high-temperature annealing in UHV. Large (>500 nm) atomically flat areas are occasionally observed. More typical, however, is terrace morphology with square edges and 5.9 ± 0.2 Å step heights such as the 400 $\times140$ nm^2 region shown in Fig. 1(a), where five terrace levels can be seen. The terrace edges are highly aligned along the *b* and *c* directions. The step height corresponds closely with half the unit cell height, which is $(a/2)\sin\beta$ =5.94 Å, because the *a* vector is not the surface normal. At higher resolution [Fig. 1(b)] we observe additional very small terraces and two more step heights of 1.5 and 4.4 Å. This suggests two possible surface terminations, labeled A and B in Fig. 1(b). Areas of the B termination constitute most of the surface, while areas of the A termination are small and confined to near step edges. While STM does not necessarily reflect the true geometric height, the measured A-B step height (0.44 nm) is significantly larger than the B-A step height (0.15 nm). Atomic resolution STM [Fig. 1(b)] reveals rows parallel to the *b* direction with spacing 5.6 ± 0.4 Å on both the B and A terminations. This spacing corresponds to the *c* lattice vector. The LEED results (Fig. 1 inset) confirm an unreconstructed surface with a single domain rectangular pattern corresponding to the unreconstructed *b* and *c* axes. Successive scans during exposure to air at 10^{-7} torr reveals that adsorbates initially attach at step edges.

A previous AFM study of cleaved β-Ga_2O_3(100) surface reported large flat areas on the micrometer scale with occasional ~6 Å steps.[8] The 20–200 nm scale rectangular morphology in Fig. 1(a) is likely induced by the high-temperature vacuum annealing used here, possibly through desorption of the volatile phase GaO. Another previous study of STM on thin Ga_2O_3 films obtained by oxidizing CoGa reveals a very long skinny island morphology with rows running down the length of the islands with spacing corresponding to the *c* axis (5.8 Å).[10,11] Stabilization of the edges by rows of Ga atoms leading to oriented edges was reported as a plausible explanation for the high aspect ratio island morphology.[10] In the single crystal case, we also observe terraces with long straight edges, but the edges run in both the *b* and *c* directions with no preference for one over the other. Therefore, we conclude that the extremely high aspect ratio islands observed in the thin film case are due to some effect of the substrate, though stabilization of the terrace edges along the *b* and *c* lattice vectors is intrinsic to Ga_2O_3. The absence of reconstruction in the 1×1 LEED pattern from the bulk crystal was also observed for the two-domain β-Ga_2O_3/CoGa film, although, in that case 1×1 β-Ga_2O_3 essentially constitutes a 2×1 reconstruction of the CoGa substrate, making the effect of the substrate difficult to separate.[10,11]

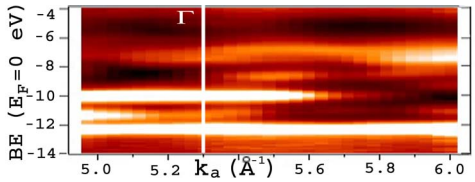

FIG. 2. (Color online) Normal emission valence band spectra taken with photon energy from 80 to 130 eV showing emission intensity (white=high intensity) as a function of binding energy and wave vector along k_a assuming an inner potential of 13 eV.

A recent theoretical study of the (100) surface presents two possible surface terminations, A and B.[7] Termination A is characterized by rows of oxygen, and termination B by rows of nearest neighbor gallium and oxygen [Fig. 1(c)]. There are two B and two A terminations per unit cell, so preferential termination at either A or B would result in a uniform step height of 5.94 Å when viewed at a large scale. The A-B step height is larger than the B-A step height, so we associate the large terraces with the B termination, and the small terraces 1.5 Å below them with the A termination. Observing larger B terminated terraces supports the theoretical result that the B termination is more energetically favorable.[7] Our results support the theoretical findings that there is no energetically favorable reconstruction of the A surface termination; no theoretical results were presented for possible B reconstructions.[7]

The electronic structure of wide gap semiconductors strongly influences the technologically useful optical properties of these systems. Yet, while theoretical electronic band structures of β-Ga_2O_3 based on density functional theory (DFT) have been available for years,[17,18] there has to our knowledge been no analogous experimental data with which to compare. Figures 2 and 3 present the experimental electronic dispersion relations along high symmetry directions, extracted from a 4D data set I (a^*, b^*, c^*, BE) obtained from ARPES. The data are plotted with respect to the reciprocal lattice vectors of the simple monoclinic unit cell of the dimensions given above.

Figure 2 shows the dispersion (photoemission intensity as function of binding energy and wave vector) plotted along the a^* vector, which is the surface normal and also called k_a. The inner potential was estimated to be 13 eV. The inner potential is difficult to determine from this experiment because the dispersion of the bands in that direction is fairly

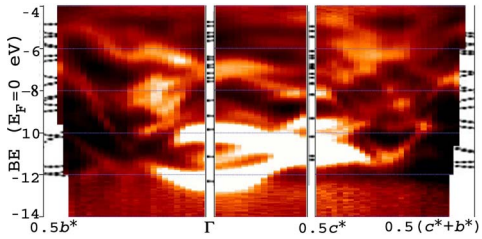

FIG. 3. (Color online) Experimental band structure along high symmetry directions b^* and c^* determined from ARPES (intensity map). Predicted band locations from published DFT calculations from Ref. 17 at Γ, the Brillouin zone boundary at 0.5 c^*, and halfway along the b^* direction from Γ and 0.5 c^*, are shown as dotted black lines for comparison. The calculated bandwidth has been scaled up from 7 eV to match the experimental width of ~7.5 eV.

small, although this also means that a relatively large error can be tolerated. A Γ point at 10 a^* occurs at k_a=5.3 Å^{-1}. From this Γ point the dispersion relations are plotted along other reciprocal lattice vectors in Fig. 3. There are a series of bright bands showing clear angular dispersion from about −4.5 to −12 eV giving an overall bandwidth of about 7.5 eV. This is in reasonable agreement with calculated band structures, which give bandwidths of about 7 eV.[17,18] Relative to these bands the crystal is highly *n*-type with the top of the bright bands located ~4.5 eV below the Fermi level. There is also a nonzero density of states above these bands consisting of localized states that show no angular dispersion. These states are probably due to crystal defects and should not be associated with the perfect crystal or compared with DFT results, though they may relate to the electrical conduction and optical properties.

The overall agreement between the experimental band structure and published DFT calculation[17,18] is quite good, but there are differences. Figure 3 compares the experimentally determined bands from Γ to $b^*/2$, from Γ to $c^*/2$, and from $c^*/2$ to $(b^*+c^*)/2$, to the DFT results at the points Γ, the Brillouin zone boundary at 0.5 c^*, and 0.5 b^* from these points. The calculated bands are stretched in energy from their original width of 7 eV to agree with the experimental width of ~7.5 eV, and aligned on the strongly emitting state at the bottom of valence band. The band locations in the two referenced calculated structures[17,18] are identical to within relevant error limits. The valence band is primarily of O 2*p* character, with negligible contribution from Ga.[17] While the absolute experimental and computed bandwidths differ, both find the bandwidth is smaller at and along the zone boundary at 0.5 c^* than at Γ by about 15%.

In general, the agreement between the experiment and the calculations is better at Γ and along the a^* and c^* directions than along the b^* direction. At the Γ point, both the calculated structures and the experimental data show bands at −12.5, −11, and −10 eV. Less intense bands are also apparent in the experiment just above and below −9 eV, which also appear in the calculations. A calculated cluster of bands between −6 and −8 eV appears as one wide band centered at −7 eV in the experiment. There is also a faint band in the experimental data near the top of valence band at the Γ point; it is difficult to compare with the wide cluster of bands predicted there. In the b^* direction the experimental data shows more dispersion than is present in the calculated structures,[17,18] which lead to decreased agreement between the experiment and theory at 0.5 b^* and 0.5(b^*+c^*) in Fig. 3. The differences are more apparent when comparing the dispersion of the bands along the b^* direction (not shown) where, for example, the bands near the bottom of the valence band at Γ at −10 and −12.5 eV come together at 0.25 b^* in the experimental data, but not until about 0.4 b^* in the calculated band structure.

In conclusion, we have presented STM, LEED, and ARPES results on bulk single crystals of the transparent wide gap semiconductor β-Ga_2O_3. STM and LEED show that the surface is well ordered and unreconstructed at the atomic scale. On a larger scale, UHV-annealed surfaces exhibit rectangular terraces with edges aligned along the *b* and *c* axes. The most prevalent surface termination is identified to be the "B" surface, with gallium and oxygen, with the oxygen terminated "A" surface observed in small regions. Comparison of ARPES with band structures from DFT results show excellent agreement at the Γ point, except for the experimental bandwidth being ~6% larger, and good agreement from Γ along c^* and a^*. The dispersion along the b^* direction is underestimated by the calculations.

Work was supported in Seattle by the NSF under Grant No. DMR-0605601, at the ALS by the DOE under Contract No. DE-AC02-05CH11231. T.C.L. and E.N.Y. acknowledge fellowship support, TCL–IGERT Fellowship NSF/NCI DGE 0504573 through the Center for Nanotechnology at the UW, ENY-IBM Fellowship.

[1] V. E. Henrich and P. A. Cox, *The Surface Science of Metal Oxides* (Cambridge University Press, Cambridge, 1994).
[2] U. Diebold, Surf. Sci. Rep. **48**, 53 (2003).
[3] C. Woll, Prog. Surf. Sci. **82**, 55 (2007).
[4] M. Batzill and U. Diebold, Prog. Surf. Sci. **79**, 47 (2005).
[5] M. Orita, H. Ohta, M. Hirano, and H. Hosono, Appl. Phys. Lett. **77**, 4166 (2000).
[6] M. Zinkevich and F. Aldinger, J. Am. Ceram. Soc. **87**, 683 (2004).
[7] V. M. Bermudez, Chem. Phys. **323**, 193 (2006).
[8] E. G. Villora, K. Shimamura, K. Aoki, and N. Ichinose, J. Cryst. Growth **270**, 462 (2004).
[9] S. Ohira, N. Arai, T. Oshima, and S. Fujita, Appl. Surf. Sci. **254**, 7838 (2008).
[10] M. Eumann, G. Schmitz, and R. Franchy, Appl. Phys. Lett. **72**, 3440 (1998).
[11] G. Schmitz, P. Grassmann, and R. Franchy, J. Appl. Phys. **83**, 2533 (1998).
[12] E. Villora, K. Shimamura, Y. Yoshikawa, T. Ujiie, and K. Aoki, Appl. Phys. Lett. **92**, 202120 (2008).
[13] M. Fleischer, L. Hollbauer, E. Born, and H. Meixner, J. Am. Ceram. Soc. **80**, 2121 (1997).
[14] M. Bartic, C.-I. Baban, H. Suzuki, M. Ogita, and M. Isai, J. Am. Ceram. Soc. **90**, 2879 (2007).
[15] E. G. Villora, K. Shimamura, K. Aoki, and K. Kitamura, Thin Solid Films **500**, 209 (2006).
[16] N. Ueda, H. Hosono, R. Waseda, and H. Kawazoe, Appl. Phys. Lett. **70**, 3561 (1997).
[17] K. Yamaguchi, Solid State Commun. **131**, 739 (2004).
[18] H. He, M. A. Blanco, and R. Pandey, Appl. Phys. Lett. **88**, 261904 (2006).